Contrib Mineral Petrol (1993) 114:289–295

Contributions to Mineralogy and Petrology

Buoyancy-driven propagation of an isolated fluid-filled crack in rock: implication for fluid transport in metamorphism

Yoshito Nakashima

Institute of Applied Physics, University of Tsukuba, Tsukuba, Ibaraki 305, Japan

Received May 30, 1992 / Accepted January 4, 1993

Abstract. A new model for upward transport of buoyant fluid released during metamorphism is proposed. The model is fluid transport by buoyancy-driven propagation of isolated fluid-filled cracks. The mechanical behavior of a two-dimensional, isolated, vertical, and fluid-filled crack in impermeable rock is investigated using linear fracture mechanics and fluid dynamics. The results show that steady-state crack propagation which causes long-distance transport of the fluid occurs when the vertical cross-sectional area of the crack exceeds a critical value. Propagation velocity and average thickness of the crack under the steady-state propagation regime are expressed explicitly by the following seven parameters: vertical crack length; rigidity, Poisson's ratio, and fracture toughness of the rock; fluid viscosity; density difference between the rock and the fluid; gravitational acceleration. An isolated H_2O-filled crack of vertical length 100 m, for example, propagates upwards in the crust at ~ 0.3 m/s with the average thickness ~ 0.2 mm when the following likely values are assumed: 0.1 mPa s for the H_2O viscosity; 3 MPa $m^{1/2}$ for the fracture toughness of the crustal rock. The application of the obtained results to the transport of H_2O released during metamorphism suggests that the number density of isolated cracks propagating in the crust is very low. Since the propagation velocity is high, our model is suitable particularly for fluid transport through hot quartz-rich rock where fluid-filled cracks have geologically short lifetimes.

Introduction

Aqueous fluid is released in the crust (Fyfe et al. 1978) and mantle (Tatsumi et al. 1986; Finger et al. 1989) by metamorphic dehydration. The released fluid migrates upward because its density is lower than the surrounding rock. Bickle and McKenzie (1987) and Connolly and Thompson (1989) studied fluid migration quantitatively assuming permeable flow through uniformly distributed preexisting microcracks and pores in the rock. However, the widespread occurrence of quartz and calcite veins in metamorphic belts suggests that fluid flow through highly localized open channels (veins) made by hydraulic fracturing can be an important mode of fluid migration (Fyfe et al. 1978). The fluid transport by hydraulic fracturing occurs when rock becomes less permeable by, for example, syntectonic recrystallization (Yardley 1986). Bailey (1990) also showed that the hydraulic fracturing mode was more dominant than the permeable flow mode above the brittle-ductile transition zone of the continental crust (this was because the thermally activated permeability was low owing to the low temperature). Walther and Orville (1982) and Walther and Wood (1984) discussed fluid transport by hydraulic fracturing. They considered fluid flow through stationary open cracks (veins) fractured hydraulically. A new model to deal with propagating (i.e. non-stationary) fluid-filled cracks is proposed in the present paper. In the new model upward fluid transport results from the buoyancy-driven propagation of isolated fluid-filled cracks. This model is applicable to impermeable or less permeable situations (e.g. upward fluid transport to the Earth's surface from a region where fluid is being released by metamorphism through overlying impermeable cap rock). To develop the model, statics and dynamics of an isolated fluid-filled crack in rock are considered using linear fracture mechanics and simple fluid dynamics. Notation is listed in Table 1.

Statics

Static stability of a crack in rock after fluid (H_2O, CO_2, magma, molten iron etc.) injection is examined in this section. The crack is termed "stable" in this paper when neither closure of the crack nor fracture of the rock occurs. The problem of the static stability of an isolated fluid-filled crack was investigated by Weertman (1971a), Secor and Pollard (1975), Pollard (1976), and Maaløe (1987). However, an important problem, the behavior of an unstable crack, has not been addressed. The major purpose of this section is to solve this problem.

Table 1. Notation list

Quantity	Meaning
$2a$	Vertical crack length
A	Dimensionless a
b	Vertical cross-sectional area of a crack
B	Dimensionless b
e	Parameter of a crack shape
f	Upward fluid flux
F_{buoy}	Total buoyancy of fluid in a crack
F_{elast}	Total elastic support by rock deformation
F_{vis}	Total viscous support by fluid motion
g	Gravitational acceleration
G	Rigidity of rock
$2h$	Crack thickness
H	Dimensionless h
$2h_{\text{AV}}$	Average crack thickness
K	Stress intensity factor at a crack tip
K_c	Fracture toughness of rock
N	Number density of propagating cracks
P	Pressure
P_{ex}	Excess pressure in fluid
P_0	Excess pressure at a crack center
P_1	Excess pressure gradient in fluid
V	Propagation velocity of a crack
x	Horizontal coordinate
y	Vertical coordinate
Y	Dimensionless y
ρ_f	Density of fluid
ρ_r	Density of rock
$\delta\rho$	$\rho_r - \rho_f$
η	Viscosity of fluid
ν	Poisson's ratio of rock
τ	Viscous shear stress on a crack wall

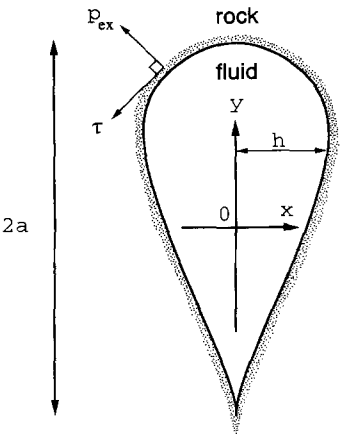

Fig. 1. Vertical cross section of an isolated fluid-filled crack in rock. The half thickness, h, is exaggerated in comparison with the vertical crack length, $2a$. After the fluid injection, the vertical cross-sectional area (b) remains constant. The origin of the x-y coordinate system is located at the crack center. The stress on the crack wall consists of τ (shear stress) and P_{ex} (normal stress). The direction of the gravity is the negative y direction

Consider a two-dimensional, preexisting, and vertical crack which is isolated from a fluid reservoir and has a vertical length of $2a$. The crack is injected with a volume of fluid, so that the cross-sectional area is b (Fig. 1). We analyze the mechanical stability of the crack (specified by a and b) after the fluid injection. Initiation problems (i.e. how a crack of length $2a$ forms and how the crack is injected with fluid from a fluid reservoir) are not considered in the present study; they have been treated by Nishiyama (1989) and Y. Nakashima (submitted).

The following assumptions are made for the analysis: (i) the rock is isotropic, homogeneous, impermeable, and elastic; (ii) the fluid is homogeneous and incompressible; (iii) the pressure field $P(x, y)$ in the rock is lithostatic before the fluid injection; (iv) the rock is governed by linear fracture mechanics of plane strain (effects of plastic deformation of the rock are neglected); (v) the crack is deep in the Earth (effects of the Earth's stress free surface are ignored); (vi) there are no chemical reactions or phase transitions (effects of stress corrosion cracking and solidification of the fluid are neglected); (vii) the interfacial energy between the rock and the fluid is small compared with the buoyancy of the fluid.

The assumption (iii) leads to Eq. (1):

$$P(\pm\infty, y) = P(\pm\infty, 0) - \rho_r g y \tag{1}$$

for $-\infty < y < \infty$ where ρ_r and g denote the density of the rock and the gravitational acceleration, respectively. Equation (1) remains valid even after the fluid injection into the crack. Since the fluid in the crack is static, the pressure field P in the fluid is given by

$$P(0, y) = P(0, 0) - \rho_f g y \tag{2}$$

for $-a < y < a$ where ρ_f is the density of the fluid. Therefore the excess pressure P_{ex} which causes the deformation of the crack wall is derived from (1) and (2):

$$P_{\text{ex}}(y) = P(0, y) - P(\pm\infty, y) = P_0 + \delta\rho g y \tag{3}$$

for $-a < y < a$ where $P_0 = P_{\text{ex}}(0) = P(0, 0) - P(\pm\infty, 0)$ and $\delta\rho = \rho_r - \rho_f$. Although $\delta\rho$ is positive for the fluid release during metamorphism, negative $\delta\rho$ cases are also considered as a generality in this section; Stolper et al. (1981) suggest that basic melt generated in the deep mantle becomes denser than residual peridotite. The $\delta\rho$ is also negative for the Earth's core formation by the propagation of cracks filled with molten iron (Stevenson 1981).

According to Weertman (1971a), Secor and Pollard (1975), and Maaløe (1987), the half thickness $h(y)$ of the crack caused by the linear excess pressure $P_{\text{ex}}(y)$ is given by

$$h(y) = \left(\frac{1-\nu}{G}\right) P_0 \sqrt{a^2 - y^2}\left(1 + \frac{\delta\rho g y}{2P_0}\right) \tag{4}$$

for $-a < y < a$ where ν and G denote Poisson's ratio and rigidity of the rock, respectively [in the case of plane stress, the coefficient $(1-\nu)$ in (4) should be replaced with $(1+\nu)^{-1}$]. It is convenient to introduce a non-dimensional half thickness H and vertical coordinate Y: $h = H(1-\nu)aP_0/G$ and $y = aY$. As a result Eq. (4) can be rewritten as

$$H(Y) = \sqrt{1 - Y^2}(1 + eY) \tag{5}$$

for $-1 < Y < 1$ where

$$e = \frac{\delta\rho g a}{2P_0}. \tag{6}$$

Equation (5) shows that the non-dimensional number e is the only parameter which governs the crack shape. The

vertical cross-sectional forms of the crack for $e = 0$, ± 0.5, ± 1, and ± 3 are shown in Fig. 2. When $|e| > 1$, the solution (5) is not physically real because the crack walls overlap one another. Thus the stability condition against the overlap is

$$|e| \leq 1. \tag{7}$$

Another condition for stability arises from linear fracture mechanics: the stress intensity factor K at a crack tip cannot exceed a critical value K_c. The K_c value is a characteristic quantity of a brittle material and termed "the fracture toughness of mode I". The stress intensity factors at the upper ($y = a$) and lower ($y = -a$) crack tips are given by Secor and Pollard (1975) and Ishida (1987):

$$K_{y=\pm a} = P_0\sqrt{\pi a} \pm \frac{\delta\rho g a}{2}\sqrt{\pi a}. \tag{8}$$

Different conventions are used by other authors for K, which differs by the factor $\pi^{1/2}$ or $(2\pi)^{1/2}$. If the fracturing of the rock at the crack tips is to be avoided, the following condition must be satisfied:

$$K_{y=\pm a} \leq K_c. \tag{9}$$

As a result two conditions (7) and (9) for the static stability are obtained.

Since the fluid is considered to be incompressible, the cross-sectional area b (*two-dimensional volume* of the fluid) must remain constant during fracturing of the rock and/or crack closure. Thus it is useful to express b by (10):

$$b = 2\int_{-a}^{a} h(y)\,dy = \left(\frac{1-\nu}{G}\right)\pi P_0 a^2. \tag{10}$$

Quantities a and P_0 will vary and be related to each other by (10) during fracturing and/or crack closure. Let us make an approximation that the crack shape is a rectangle (length $2a$, thickness $2h_{AV}$). Since the area of the rectangle equals b, the average half thickness h_{AV} of the crack is given by

$$h_{AV} = \frac{b}{4a}. \tag{11}$$

The stability criteria can now be expressed in terms of a and b by the substitution of (6), (8), and (10) into (7) and (9) to obtain:

$$b \geq \left(\frac{1-\nu}{G}\right)\frac{\pi|\delta\rho|g}{2}a^3 \tag{12.1}$$

$$b \leq \left(\frac{1-\nu}{G}\right)a\sqrt{\pi a}\left(K_c \pm \frac{\delta\rho g a}{2}\sqrt{\pi a}\right). \tag{12.2}$$

Introducing the non-dimensional half length A and the non-dimensional area B of the crack, we rewrite (12.1) and (12.2) as

$$B \geq A^3 \tag{13.1}$$

$$B \leq A\sqrt{A}(1 \pm A\sqrt{A}) \tag{13.2}$$

where

$$a\sqrt{a} = \frac{2K_c}{\sqrt{\pi}|\delta\rho|g}A\sqrt{A} \tag{14.1}$$

$$b = 2\left(\frac{1-\nu}{G}\right)\frac{K_c^2}{|\delta\rho|g}B. \tag{14.2}$$

The stability conditions (7) and (9) are now represented by two inequalities (13.1) and (13.2). The substitution of (6), (14.1), and (14.2) into (10) yields

$$B = \frac{A^3}{|e|}. \tag{15}$$

The described statics are summarized in Fig. 3 as a stability diagram. It should be noted from the figure that the upward (downward) steady-state crack propagation driven by the positive (negative) buoyancy of the fluid occurs if $B > 0.25$.

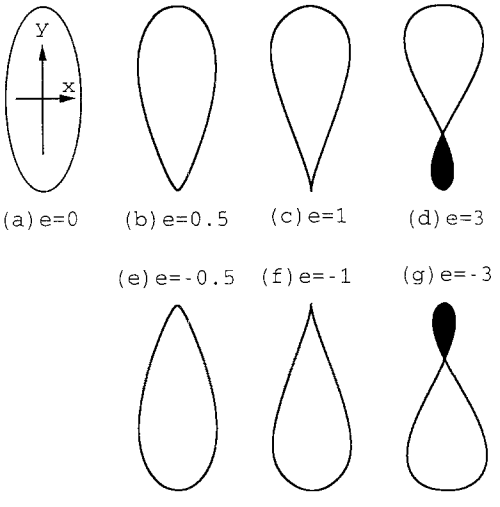

Fig. 2a–g. Cross-sectional shapes of a static crack for various values of e. Calculated by (4). The horizontal scale is exaggerated. The overlapped parts of the crack walls due to negative $h(y)$ are *shaded*: **a** Ellipse; **b** $P_{ex}(-a) = 0$; **c** cusped at the lower crack tip; **d** overlap near $y = -a$; **e** $P_{ex}(a) = 0$; **f** cusped at the upper crack tip; **g** overlap near $y = a$

Dynamics

When the non-dimensional cross-sectional area B of a fluid-filled crack is greater than 0.25, the crack will migrate through the rock. Although Weertman (1971b), Maaløe (1987), and Takada (1990) studied the buoyancy-driven propagation of an isolated crack, the dynamics have not been elucidated. The purpose of this section is to describe the propagation dynamics of an isolated fluid-filled crack whose B is greater than 0.25. The propagation velocity V, the average half thickness h_{AV}, and the vertical cross-sectional area b will be represented by means of the half length a.

Consider a two-dimensional isolated vertical crack propagating in rock (Fig. 1). The assumptions in addition to (i)–(vii) of the previous section are as follows: (viii) the upward steady-state propagation driven by the positive buoyancy of the fluid is assumed [$\delta\rho > 0$ and the crack propagates upward at a constant speed V and a constant shape $h(y)$]; (ix) the fluid is homogeneous and Newtonian (effects of fluid degassing near the crack tip are neglected); (x) the fluid flow is a steady laminar flow between two

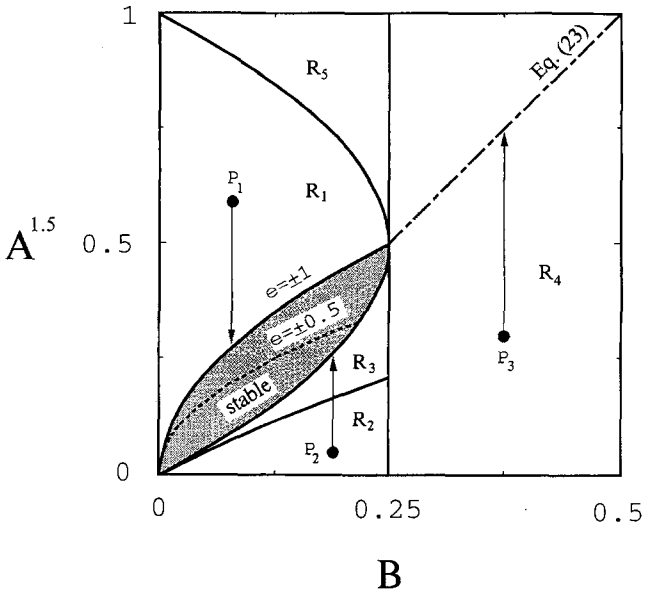

Fig. 3. Stability diagram of a two-dimensional, isolated, vertical, and fluid-filled crack. *Heavy solid parabolas* are drawn by (13.1) and (13.2). The B-A plane is divided into six regions by the *heavy solid parabolas* and *lines*: one *stable* region, *shaded*; three regions, R_1, R_2, and R_3, where transient fracturing or shrinkage occurs; one region, R_4 where steady-state propagation occurs; one region, R_5, which is not realizable. The following points can be made: (1) A crack in the stable region neither propagates nor shrinks because all stability conditions (13.1) and (13.2) are satisfied. Equation (15) for $e = \pm 0.5$ is plotted for reference by a *dotted parabola*. (2) Shrinkage of the crack length occurs in the region R_1. For example, suppose a situation of point P_1 achieved for an instant by fluid injection. The state P_1 is unstable because $|e| > 1$. Thus the following phenomenon occurs. If $\delta\rho$ is negative (positive), the crack is squeezed at the upper (lower) crack tip and shrinks. The state of the crack shifts along the indicated *arrow* keeping B constant. The crack ceases shrinking after the state of the crack reaches the parabola of $e = -1$ ($e = 1$). The crack remains stationary after this transient shrinkage. (3) Elongation of the crack length by fracturing takes place in the regions of R_2 and R_3. If the state of point P_2 is given as an initial condition by fluid injection, the following will occur because P_2 does not satisfy (13.2). The crack elongates both upwards and downwards keeping B constant while the state of the crack is located in the region R_2. After the state of the crack enters the region R_3, the crack elongates only from the upper (lower) crack tip if $\delta\rho$ is positive (negative). The elongation ends when the state of the crack arrives at the margin of the stable region. This instability is also transient. (4) Steady-state crack propagation occurs when $B > 0.25$. The state P_3 is unstable and shifts along the *arrow* to reach the *dash-dotted line* of equation (23). Since there is no stable solution for a crack of $B > 0.25$, the crack propagation is not transient but permanent. (5) The region R_5 is not realizable. This is because it is out of the *shaded* "stable" region and the line (23) does not enter R_5. Consider an example of crack growth by consecutive fluid injection into an infinitesimal crack. The state of the crack starts from $(B, A^{1.5}) \approx (0, 0)$ and shifts along the parabola $(B = A^{1.5} - A^3)$ to reach $(B, A^{1.5}) = (0.25, 0.5)$. Further fluid injection will lead the crack to the regime of the steady-state propagation (the state will shift along the line (23)). Consider another example (crack shrinkage by consecutive fluid extraction from a largest stable crack). The state of the crack starts from $(B, A^{1.5}) = (0.25, 0.5)$ and shifts along the parabola $(B = A^3)$ to reach $(B, A^{1.5}) = (0, 0)$

parallel walls (plane Poiseuille flow approximation by Weertman 1971b). The critical value of the Reynolds number $1.5\rho_f V h_{AV}/\eta$ (η is the fluid viscosity) for the laminar regime is about 6,000 (Nishioka et al. 1975).

It follows from (x) that the excess pressure P_{ex} within the moving fluid is linear with respect to y:

$$P_{ex}(y) = P_0 + P_1 y \tag{16}$$

where P_0 and P_1 are unknown constants and for $-a < y < a$. Thus crack shape $h(y)$ and stress intensity factors K at $y = \pm a$ are given by (17) and (18).

$$h(y) = \left(\frac{1-\nu}{G}\right) P_0 \sqrt{a^2 - y^2}\left(1 + \frac{P_1 y}{2P_0}\right) \tag{17}$$

$$K_{y=\pm a} = P_0\sqrt{\pi a} \pm \frac{P_1 a}{2}\sqrt{\pi a}. \tag{18}$$

The assumption (viii) requires that the crack propagates steadily by fracturing the rock at the upper crack tip and by closing the crack at the lower crack tip. Thus the stress intensity factors at the crack tips satisfy (19) and (20):

$$K_{y=a} = K_c \tag{19}$$

$$K_{y=-a} = 0. \tag{20}$$

Equation (20) indicates that an ascending crack has a cusped tail which already appeared in (c) and (f) of Fig. 2.

From the assumption (v), it follows that the rate of the crack propagation will be controlled by the rate with which the fluid reaches the crack tip. Therefore V is controlled by a Poiseuille flow between parallel walls:

$$V = \frac{h_{AV}^2}{3\eta}(\delta\rho g - P_1). \tag{21}$$

In the above equations, unknown quantities are P_0, P_1, b, h_{AV}, and V. They are expressed explicitly by combining (10), (11), and (18)–(21):

$$P_0 = \frac{K_c}{2\sqrt{\pi a}} \tag{22.1}$$

$$P_1 = \frac{K_c}{a\sqrt{\pi a}} \tag{22.2}$$

$$b = \left(\frac{1-\nu}{G}\right)\frac{K_c a\sqrt{\pi a}}{2} \tag{22.3}$$

$$h_{AV} = \left(\frac{1-\nu}{G}\right)\frac{K_c\sqrt{\pi a}}{8} \tag{22.4}$$

$$V = \frac{1}{192\eta}\left(\frac{1-\nu}{G}\right)^2 K_c^2 \pi a\left(\delta\rho g - \frac{K_c}{a\sqrt{\pi a}}\right) \tag{22.5}$$

for

$$a \geq \left(\frac{K_c}{\delta\rho g\sqrt{\pi}}\right)^{\frac{2}{3}}$$

(i.e. for $A^{1.5} \geq 0.5$ or $B \geq 0.25$). The crack profile $h(y)$ is given by (22.1), (22.2), and (17). The substitution of (14.1) and (14.2) into (22.3) yields non-dimensional equation (23) which is plotted in Fig. 3:

$$B = \frac{A\sqrt{A}}{2}. \tag{23}$$

Two points are noted from the results (22.1)–(22.5): (1) When the crack is stationary (i.e. $V = 0$), $P_1 = \delta\rho g$. As V increases, P_1 decreases. Thus the assumption that $P_1 = \delta\rho g$ (Maaløe 1987) in a propagating crack is invalid. (2) Parameters h_{AV} and V depend on K_c essentially when a fluid-filled crack is isolated from a fluid reservoir. In

contrast to the isolated case, Lister (1990) found their independence from K_c when a crack propagates maintaining massive fluid injection from a reservoir. This is an essential contrast caused by connection with a reservoir.

The total buoyancy F_{buoy} of the fluid confined in the crack is given by (24) using (22.3):

$$F_{buoy} = \delta\rho g b = \left(\frac{1-\nu}{G}\right)\frac{K_c \delta\rho g a\sqrt{\pi a}}{2}. \tag{24}$$

The total elastic support F_{elast} by the surrounding rock is:

$$F_{elast} = -2\int_{-a}^{a}(P_0 + P_1 y)\left(\frac{dh}{dy}\right)dy = \left(\frac{1-\nu}{G}\right)\frac{K_c^2}{2} \tag{25}$$

where $h(y)$ is given by (17). Considering a Poiseuille flow approximation, we obtain the total viscous drag force F_{vis}:

$$F_{vis} = 2\int_{-a}^{a}\tau dy = \left(\frac{1-\nu}{G}\right)\frac{\delta\rho g K_c a\sqrt{\pi a}}{2} - \left(\frac{1-\nu}{G}\right)\frac{K_c^2}{2} \tag{26}$$

where τ is the viscous shear stress applied on the crack wall. Equations (24), (25), and (26) satisfy the following force balance:

$$F_{buoy} = F_{elast} + F_{vis}. \tag{27}$$

Equation (27) shows that total buoyancy of the fluid is exactly equal to the sum of (1) the elastic stress caused by the deformation of the crack wall and (2) the viscous drag force generated at the crack wall. The force balance is satisfied although the simple approximation (x) for the fluid flow is made.

The contributions of F_{elast} and F_{vis} to F_{buoy} are calculated by (14.1), (24), (25), and (26):

$$\frac{F_{elast}}{F_{buoy}} = \frac{1}{2A\sqrt{A}} \tag{28.1}$$

$$\frac{F_{vis}}{F_{buoy}} = 1 - \frac{1}{2A\sqrt{A}} \tag{28.2}$$

for $A^{1.5} > 0.5$. Equations (28.1) and (28.2) are the fractions of the respective forces with respect to the total buoyancy force. They show that the viscous contribution (28.2) becomes more dominant with increasing A (i.e. with increasing V).

Discussion

Results obtained in the previous section will be applied to the upward transport of H_2O released during metamorphism. We assume $G = 44$ GPa, $g = 9.8\ m/s^2$, and $\nu = 0.25$. These values are estimated by Dziewonski and Anderson (1981) for the crust (depth 15.0–24.4 km). Values for ρ_f and $\delta\rho$ are taken to be 1,000 kg/m^3 and 2,000 kg/m^3, respectively. Atkinson and Meredith (1987) reviewed experimental K_c data acquired under low temperatures (room temperature $\sim$700 K) and low confining pressures (0–100 MPa): for example, K_c of basic rock ranges from 0.84 to 3.75 MPa m$^{1/2}$. On the basis of this review, 3 and 0.3 MPa m$^{1/2}$ are taken as the upper and lower limits on K_c. The upper and lower limits of the H_2O viscosity η are taken as 1 and 0.1 mPa s, respectively (Walther and Orville 1982).

The largest possible stable crack filled with H_2O must satisfy $(B, A^{1.5}) = (0.25, 0.5)$ as shown in Fig. 3. By the substitution of $(B, A^{1.5}) = (0.25, 0.5)$ and the assumed physical parameters into (14.1), (14.2), and (11), the parameters $2a$ and $2h_{AV}$ are found to be 8.4–39 m and 0.0046–0.1 mm, respectively. The spread of the calculated values comes from the ambiguity of K_c. If the crack is not vertical but inclined at an angle θ, in the calculation of $2a$ and $2h_{AV}$, g in (14.1) and (14.2) should be replaced with $g\cos\theta$. The currently accepted hypothesis for vein formation in low-grade metamorphic rock is the crack-seal mechanism (repeated formation of veinlets formed by mineral precipitation in a stable fluid-filled crack) by Ramsay (1980). Suppose that a stable vertical crack is formed by a horizontally tensile tectonic stress. The crack is injected with fluid derived from the surrounding rock and mineral precipitation starts in the crack to form a veinlet. If the crack grows to satisfy $B > 0.25$, the fluid will escape from the crack by the buoyancy-driven propagation. Since the crack will be closed by this fluid escape, no further precipitation will occur. Thus our crack model suggests that the typical thickness of the veinlet is less than $2h_{AV}$ of the largest stable crack. Ramsay (1980) and Cox and Etheridge (1983) reported that the typical thickness of each veinlet was 0.01–0.04 mm. The reported value may be a consequence of the static stability of an isolated fluid-filled crack.

Propagation velocity V and average half thickness h_{AV} of an isolated H_2O-filled crack are shown in Figs. 4 and 5. Two points are illustrated in these figures:

1. The propagation velocity is high: for example, V for $a = 50$ m ranges from 0.41 mm/s = 35 m/day to 0.32 m/s = 28 km/day. The high velocity suggests that propagation of H_2O-filled cracks could be effective in upward H_2O transport during metamorphism.
2. The propagating crack is thin: the smallest h_{AV} ($a = 4.2$ m and $K_c = 0.3$ MPa m$^{1/2}$) in Fig. 5 is 2.3×10^{-3} mm. Even the smallest is substantially wider than the minimum width (10^{-5} mm) estimated by Walther and Orville (1982).

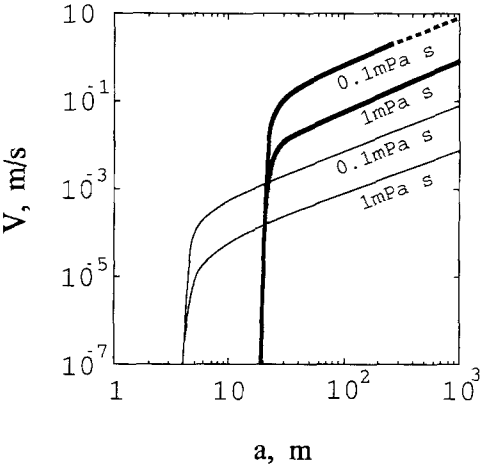

Fig. 4. Steady-state propagation velocity V calculated by (22.5). *Light curves*, $K_c = 0.3$ MPa m$^{1/2}$; *heavy curves*, $K_c = 3$ MPa m$^{1/2}$. The H_2O viscosity is indicated. Equation (22.5) breaks down on the *dotted curve* because the Reynolds number exceeds the critical value (6,000)

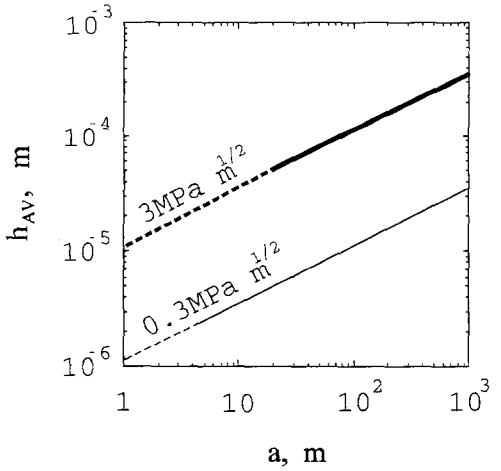

Fig. 5. Average half thickness h_{AV} calculated by (22.4). K_c is indicated. Equation (22.4) breaks down on the *dotted lines* because the crack is stationary (i.e. $B \leq 0.25$)

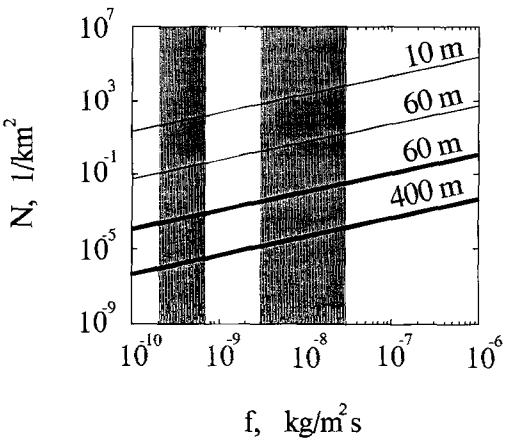

Fig. 6. Number density N calculated by (29) for $\eta = 0.1$ mPa s. *Light lines*, $K_C = 0.3$ MPa m$^{1/2}$; *heavy lines*, $K_C = 3$ MPa m$^{1/2}$. The uniform vertical length $2a$ is indicated. The ranges of f calculated by dehydration models for subducting slabs (Peacock 1990) and for regional metamorphism (Connolly and Thompson 1989) are shown by the *shaded bands*

Our model can deal with fluid transport through impermeable rock where permeable flow models are useless. Consider impermeable cap rock overlying a dehydration zone where H_2O is being released. Free H_2O is transported at a constant flux f from the dehydration zone to the Earth's surface through the cap rock. The number density N of isolated H_2O-filled cracks propagating in the cap rock can be estimated by our model. The following assumptions are made for simplicity: (1) the released H_2O is transported in the cap rock by a group of H_2O-filled cracks of uniform vertical length $2a$; (2) no mechanical interaction between cracks (e.g. collision) occurs. On the basis of the law of mass conservation, N is expressed by

$$N = \frac{f}{bV\rho_f} \tag{29}$$

where b and V are given by (22.3) and (22.5), respectively. The number density N is plotted against f in Fig. 6. The flux f caused by dehydration was estimated at 9.4×10^{-9} kg/m^2 s (Walther and Orville 1982) or $2 \sim 7 \times 10^{-10}$ kg/m^2 s (Connolly and Thompson 1989) for regional metamorphism and at 6.6×10^{-9} kg/m^2 s (Walther and Wood 1984) for contact metamorphism. As for the dehydration of subducting slabs, the typical f ranges from 3×10^{-9} kg/m^2 s to 3×10^{-8} kg/m^2 s (Peacock 1990). Since N depends on a and K_c strongly as shown in Fig. 6, it is difficult to estimate N precisely. However Fig. 6 suggests that the number density of H_2O-filled cracks propagating in the crust is very low. This is a consequence of high V and the low production rate of H_2O.

Our model is suitable particularly for the fluid transport through hot quartz-rich rock where fluid-filled cracks have geologically short lifetimes. Fluid-filled cracks in hot rock change their shapes by healing driven by the interfacial energy between the rock and the fluid (Roedder 1984). This crack healing results in the formation of secondary fluid inclusions in planar arrays. Smith and Evans (1984) carried out healing experiments of fluid-filled microcracks in quartz; the results indicate that the healing of fluid-filled microcracks in quartz ends within geologically short time (e.g. a few days) at temperatures of about 500 K or greater. Thus it is difficult to transport massive fluid by permeable flow through *stationary* fluid-filled microcracks in the deep quartz-rich crust. On the other hand, our *propagating* crack model can transport massive fluid through such hot rock. For example, consider a propagating fluid-filled crack of $a = 50$ m. The duration of the contact of the fluid and a portion of the surrounding rock is $2a/V$ which is estimated at 5 minutes – 3 days from Fig. 4. The estimated duration is much shorter than (or comparable to) the characteristic time for healing. Hence probably the crack healing is not effective in a fast propagating crack (if the healing is effective, the single long crack of $a = 50$ m will be divided into numerous fluid inclusions isolated from one another and cannot propagate). The model presented in this paper gives a physical basis for the upward fluid transport through hot quartz-rich rock.

Acknowledgments. The author thanks T. Hirata, T. Ogawa, and K. Kurita for many stimulating and encouraging discussions. He also thanks J.A.D. Connolly and M. Kumazawa for helpful comments.

References

Atkinson BK, Meredith PG (1987) Experimental fracture mechanics data for rocks and minerals. In: Atkinson BK (ed) Fracture mechanics of rock. Academic Press, London, pp 477–525

Bailey RC (1990) Trapping of aqueous fluids in the deep crust. Geophys Res Lett 17:1129–1132

Bickle MJ, McKenzie D (1987) The transport of heat and matter by fluids during metamorphism. Contrib Mineral Petrol 95:384–392

Connolly JAD, Thompson AB (1989) Fluid and enthalpy production during regional metamorphism. Contrib Mineral Petrol 102:347–366

Cox SF, Etheridge MA (1983) Crack-seal fibre growth mechanisms and their significance in the development of oriented layer silicate microstructures. Tectonophysics 92:147–170

Dziewonski AM, Anderson DL (1981) Preliminary reference Earth model. Phys Earth Planet Inter 25:297–356

Finger LW, Ko J, Hazen RM, Gasparik T, Hemley RJ, Prewitt CT, Weidner DJ (1989) Crystal chemistry of phase B and an anhydrous analogue: implications for water storage in the upper mantle. Nature 341:140–142

Fyfe WS, Price NJ, Thompson AB (1978) Fluids in the Earth's crust. Elsevier, Amsterdam

Ishida M (1987) Stress intensity factor of a crack under polynomial distribution of stress in an infinite plate. In: Murakami Y (ed) Stress intensity factors handbook, vol 1. Pergamon Press, Oxford, p 189

Lister JR (1990) Buoyancy-driven fluid fracture: the effects of material toughness and of low-viscosity precursors. J Fluid Mech 210:263–280

Maaløe S (1987) The generation and shape of feeder dykes from mantle sources. Contrib Mineral Petrol 96:47–55

Nishioka M, Iida S, Ichikawa Y (1975) An experimental investigation of the stability of plane Poiseuille flow. J Fluid Mech 72:731–751

Nishiyama T (1989) Kinetics of hydrofracturing and metamorphic veining. Geology 17:1068–1071

Peacock SM (1990) Numerical simulation of metamorphic pressure-temperature-time paths and fluid production in subducting slabs. Tectonics 9:1197–1211

Pollard DD (1976) On the form and stability of open hydraulic fractures in the Earth's crust. Geophys Res Lett 3:513–516

Ramsay JG (1980) The crack-seal mechanism of rock deformation. Nature 284:135–139

Roedder E (1984) Changes in inclusions after trapping. In: Ribbe PH (ed) Fluid inclusions (Reviews in Mineralogy 12). Mineral Soc Am, Washington, DC, pp 47–77

Secor DT, Pollard DD (1975) On the stability of open hydraulic fractures in the Earth's crust. Geophys Res Lett 2:510–513

Smith DL, Evans B (1984) Diffusional crack healing in quartz. J Geophys Res 89:4125–4135

Stevenson DJ (1981) Models of the Earth's core. Science 214:611–619

Stolper E, Walker D, Hager BH, Hays JF (1981) Melt segregation from partially molten source regions: the importance of melt density and source region size. J Geophys Res 86:6261–6271

Takada A (1990) Experimental study on propagation of liquid-filled crack in gelatin: shape and velocity in hydrostatic stress condition. J Geophys Res 95:8471–8481

Tatsumi Y, Hamilton DL, Nesbitt RW (1986) Chemical characteristics of fluid phase released from a subducted lithosphere and origin of arc magmas: evidence from high-pressure experiments and natural rocks. J Volcanol Geothermal Res 29:293–309

Walther JV, Orville PM (1982) Volatile production and transport in regional metamorphism. Contrib Mineral Petrol 79:252–257

Walther JV, Wood BJ (1984) Rate and mechanism in prograde metamorphism. Contrib Mineral Petrol 88:246–259

Weertman J (1971a) Theory of water-filled crevasses in glaciers applied to vertical magma transport beneath oceanic ridges. J Geophys Res 76:1171–1183

Weertman J (1971b) Velocity at which liquid-filled cracks move in the Earth's crust or in glaciers. J Geophys Res 76:8544–8553

Yardley BWD (1986) Fluid migration and veining in the Connemara Schists, Ireland. In: Walther JV, Wood BJ (eds) Fluid-rock interactions during metamorphism. Springer, Berlin Heidelberg New York, pp 109–131

Editorial responsibility: J. Touret